CHIN. PHYS. LETT. Vol. 38, No. 2 (2021) 027801

Wide-Angle Ultra-Broadband Metamaterial Absorber with Polarization-Insensitive Characteristics

Peng Chen(陈鹏)[2,3], Xianglin Kong(孔祥林)[2,3], Jianfei Han(韩建飞)[1], Weihua Wang(王伟华)[1], Kui Han(韩奎)[1], Hongyu Ma(马洪宇)[2,3], Lei Zhao(赵雷)[3*], and Xiaopeng Shen(沈晓鹏)[1*]

[1]*School of Materials Science and Physics, China University of Mining and Technology, Xuzhou 221116, China*
[2]*National and Local Joint Engineering Laboratory of Internet Application Technology on Mine, China University of Mining and Technology, Xuzhou 221116, China*
[3]*School of Information and Control Engineering, China University of Mining and Technology, Xuzhou 221116, China*

(Received 21 September 2020; accepted 10 December 2020; published online 27 January 2021)

An ultra-wideband metamaterial absorber is developed, which is polarized-insensitive and angular-stable. Three layers of square resistive films comprise the proposed metamaterial. The optimal values of geometric parameters are obtained, such that the designed absorber can achieve an ultra-broadband absorption response from 4.73 to 39.04 GHz (relative bandwidth of 156.7%) for both transverse electricity and transverse magnetic waves. Moreover, impedance matching theory and an equivalent circuit model are utilized for the absorption mechanism analysis. The compatibility of equivalent circuit calculation results, together with both full-wave simulation and experimental results, demonstrates the excellent performance and applicability of the proposed metamaterial absorber.

DOI: 10.1088/0256-307X/38/2/027801

Microwave absorbers (MA), as useful tools for the absorption and dissipation of electromagnetic (EM) energy, and the suppression of the reflection and transmission of EM waves, have been widely utilized in electromagnetic shielding, wireless communication, imaging, and radar stealth technology.[1–5] In the past few decades, many significant efforts have been devoted to absorber design. Although the salisbury screen, as one of the earliest wave-absorbing materials, can be easily constructed by placing a resistance film layer on a quarter wavelength dielectric plate,[6] it has a narrow bandwidth. To obtain a wider bandwidth, both Dallenbach and pyramidal absorbers have been proposed.[7,8] However, their large volume and mass confine their potential utility in many applications.

Artificially engineered materials, so-called metamaterials, possess attractive EM properties, including the inverse Doppler effect, negative refractive index,[9] backward propagation, and electromagnetic wave cloaking.[10,11] These metamaterials are known as perfect absorbers, which means that they can obtain perfect absorption over a specific bandwidth, due to the intrinsic resonance of their elements.[12–16] In addition, they can overcome the thickness limitation of traditional quarter wavelength devices. Various works have attempted to improve their absorption and polarization insensitivity.[17–22] Windmill-shaped elements were utilized by Zhang *et al.*[23] to construct a broadband metamaterial absorber, with its resultant absorption at normal incidence measuring above 90% in the frequency range of [8.3, 17.4] GHz. Resistive films were adopted by Sheokand *et al.*[24] to develop a broadband absorber, achieving more than 90% absorptivity in the frequency range of [6.06, 14.66] GHz. Han *et al.* employed multi-layer structures to design an ultrathin and broadband metamaterial absorber, achieving broadband absorption with more than 90% efficiency from 8.37 GHz to 21 GHz.[25] Shui *et al.* reported on a flexible and thin $Ti_3C_2T_x$ sponge composite operating as broadband THz absorber, whose overall structure thickness is about 2 mm, and whose absorption efficiency was as high as 90% in the 0.3–1.65 THz frequency band.[26] Hu *et al.* demonstrated 100% light absorption at near-infrared frequencies via a subwavelength multilayer dielectric grating (SMDG) structure, covered by a graphene monolayer.[27] Nevertheless, such broadband absorbers have only been reported in high-frequency bands; designs for a simple, ultra-broadband, and wide-angle absorber in the microwave band are rare, and remain quite challenging.

In this Letter, an ultra-wideband polarized-insensitive wide-angle microwave metamaterial absorber is constructed. The multilayered structure is developed using resistance film, a dielectric substrate, and a ground-plane in order to achieve broadband microwave absorption. Impedance matching theory and the equivalent-circuit model are utilized for our absorption principle analysis. Furthermore, the design is fabricated using screen printing technology,

Supported by the Six Talent Peaks Project in Jiangsu Province (Grant No. XYDXX-072), the National Natural Science Foundation of China (Grant Nos. 61372048 and 61771226), and the Natural Science Foundation of Jiangsu Province (Grant No. BK20161186).

*Corresponding authors. Email: xpshen@cumt.edu.cn; leizhao@cumt.edu.cn
© 2021 Chinese Physical Society and IOP Publishing Ltd

and the experiments are performed to validate the performance of the proposed metamaterial absorber (MMA). The proposed metamaterial absorber provides over 90% ultra-wide absorption from 4.73 GHz to 39.04 GHz and is polarization-insensitive and robust to the incidence angle.

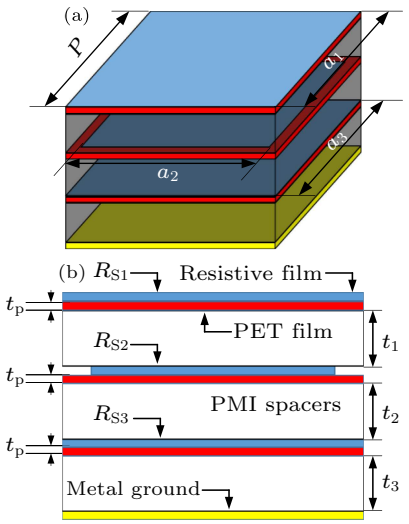

Fig. 1. Unit cell layout of the proposed MMA using multilayered resistive films: (a) perspective view, (b) side view.

The perspective and side views of the proposed broadband absorber are depicted in Fig. 1. A multilayered structure is adopted in order to realize broadband absorption at microwave frequencies. As shown in Fig. 1(a), a typical unit cell consists of three square-shaped resistive film resonators on three polyethylene glycol terephthalate (PET) films, three polymethacrylimide (PMI) spacers as the substrate, and a metal ground to prevent the transmission of the EM waves. The three square-shaped resistive film resonators, with different side lengths denoted by a_1, a_2, and a_3, are utilized as resonators, making the design polarization-insensitive and straightforward. The selected dielectric constants for PET and PMI are $3.0(1-j0.06)$ and $1.06(1-j0.005)$, respectively. The optimized unit cell size parameters are considered to be $P = 14\,\text{mm}$, $t_1 = 3\,\text{mm}$, $t_2 = 4\,\text{mm}$, $t_3 = 2\,\text{mm}$, $t_\text{p} = 0.175\,\text{mm}$, $a_1 = 14\,\text{mm}$, $a_2 = 12.5\,\text{mm}$, and $a_3 = 14\,\text{mm}$ [see Fig. 1(b)]. The surface resistance values of the three resistive films are selected to be $R_{S1} = 250\,\Omega/\square$, $R_{S2} = 450\,\Omega/\square$, and $R_{S3} = 800\,\Omega/\square$, respectively.

Numerical simulations are performed on the unit cell of the proposed design using the commercial software package, CST microwave studio. In the simulations, the unit cell's boundary conditions are adjusted in both x and y directions, while electromagnetic waves are incident perpendicularly in the negative direction of the z-axis. Figure 2 presents the absorption spectrum of the absorber. According to Fig. 2, a broadband absorption performance with more than 90% absorptivity can be attained from 4.73 GHz to 39.04 GHz at normal incidence. The proposed structure provides a relative bandwidth of 156.7%, with a central frequency of 21.9 GHz, covering the C, X, Ku, K, and Ka bands in the microwave range.

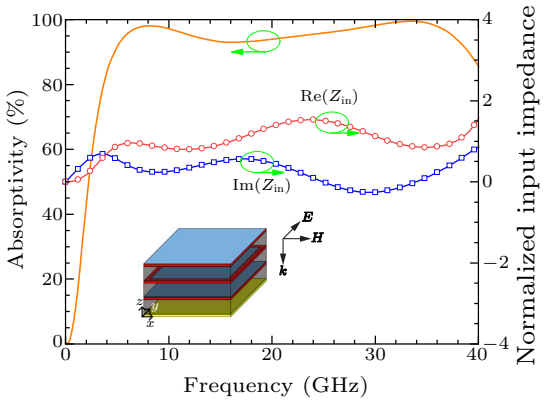

Fig. 2. Simulated absorptivity spectrum of the proposed MMA at normal incidence.

A perfect match between MMA and free space impedances must be achieved to minimize reflections and obtain a perfect absorption.[28,29] The normalized impedance of the design is calculated to further explain the broadband absorption of the proposed absorber (see Fig. 2). The real and imaginary parts of the normalized impedance are close to unity and zero, respectively. The impedance matching between MMA and free space is attained in the target frequency range, leading to a significant reduction in the backward reflection at the interface. The retrieved input impedance of MMAs can be described as

$$Z = \sqrt{\frac{(1+S_{11})^2 - S_{21}^2}{(1-S_{11})^2 - S_{21}^2}}. \tag{1}$$

This absorbing structure has been referred to as the circuit analog absorber. An equivalent circuit model is presented in Fig. 3(a) to illustrate the absorption mechanism of the proposed absorber. According to electromagnetic theory, periodic resistive films can be described via a series of RLC circuits,[30] while the dielectric layer and the bottom metal can be modeled with a transmission line and a small resistance, respectively.[31] Thus, the three-layer resistive films are described with equivalent impedances Z_1, Z_2, and Z_3, respectively. The impedances Z_4, Z_5, and Z_6 represent the dielectric layers, while the background is described by R_4. Z_in is the input impedance of the whole absorber, which can be described by means of the following equation:

$$Z_i = R_i + j\left(2\pi f L_i - \frac{1}{2\pi f C_i}\right), \quad i = 1, 2, 3. \tag{2}$$

The reflection loss of the proposed absorber can be obtained as

$$RL = 20\log 10\left|\frac{Z_\text{in} - Z_0}{Z_\text{in} + Z_0}\right|. \tag{3}$$

The circuit model is implemented, and the advanced design system software is utilized to fit the calculation

results of the circuit model with the numerical results. Table 1 gives the lumped parameters in the equivalent model. Figure 3(b) compares the absorptivity of the circuit model with that of the numerical simulation. According to Fig. 3(b), the calculated result is compatible with the simulations, validating the proposed circuit model.

Table 1. Optimal values of the equivalent circuit elements.

R_1 (Ω) 635.1	C_1 (nF) 0.8	L_1 (nH) 24.86	R_2 (Ω) 2.6
C_2 (pF) 0.01	L_2 (nH) 0.82	R_3 (Ω) 193.6	C_3 (pF) 0.12
L_3 (nH) 0.15	R_4 (Ω) 31.3	C_4 (pF) 0.06	L_4 (nH) 0.82
C_5 (nF) 602	L_5 (nH) 0.75	C_6 (nF) 1.59	L_6 (nH) 5.77

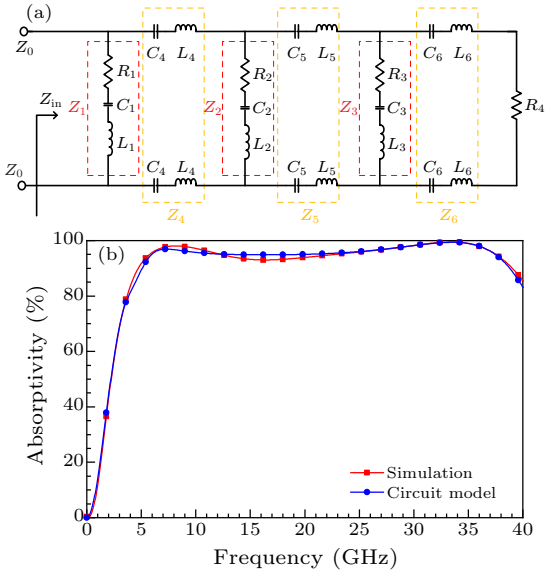

Fig. 3. (a) The Equivalent circuit model of the proposed absorber. (b) Comparison of absorptivity, calculated from the circuit model and full-wave simulations in CST.

Since the MA's absorption efficiency is generally related to the incident and polarization angles of the incident wave, the absorptivity values of the absorber for the transverse electricity (TE) and transverse magnetic (TM) polarizations under different oblique incident angles are shown in Fig. 4. For TE polarization, by increasing the incident angle from 0° to 60°, the absorptivity in the spectrum of interest decreases gradually, due to impedance mismatch at large incident angles, but its value remains more than 80%. As shown in Fig. 4(b), the absorption bandwidth for the TM polarization gradually moves towards high frequencies.

Moreover, the proposed absorber is robust to the polarization angle due to its central symmetry, as shown in Fig. 5.

Finally, Table 2 compares the proposed absorber with similar works proposed in recent years. Thickness and absorptivity, as two essential absorber indices, are calculated. The figure of merit can be expressed as $\mathrm{FoM} = d/(\lambda_L - \lambda_H)$, where d is the sample thickness and is utilized to characterize the absorber's performance[32] as compared with existing microwave absorbers.

To evaluate the absorptivity properties of the proposed structure, the square resistive film resonators are fabricated using screen-printing technology to deposit conductive ink on the polyethylene glycol terephthalate (PET) sheet; by utilizing inks with different conductivities, and adjusting the thickness of the resistive film, different resistance values can be achieved. PMI dielectric layers with different thicknesses were prepared using a foam cutting machine, and finally assembled together to prepare a complete sample. The sample has a full size of 350 mm × 350 mm, comprising 25 × 25 units [see Fig. 5(b)].

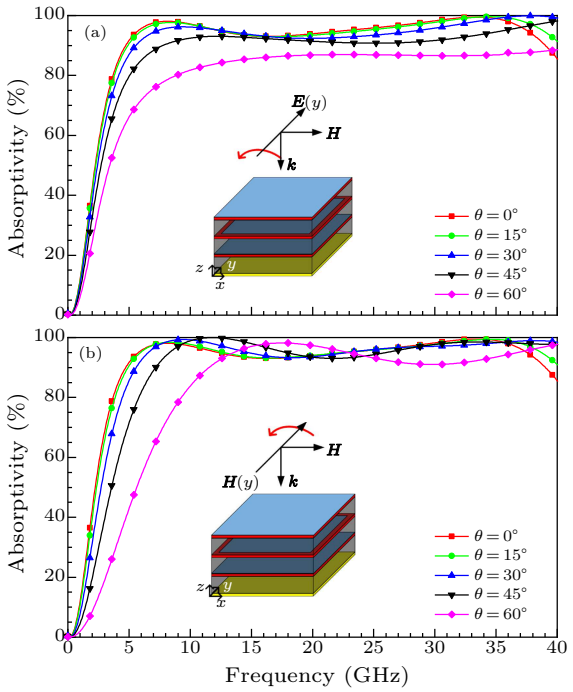

Fig. 4. Simulated absorptivity spectra for the proposed structure under incidence angles from 0° to 60° for (a) TE polarization and (b) TM polarization waves. The polarization direction and the incident angle θ are indicated in the insets.

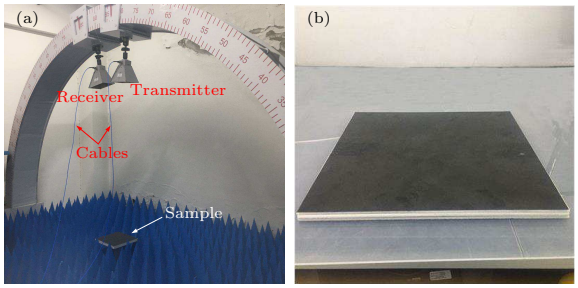

Fig. 5. (a) The whole experimental setup in a microwave chamber. (b) Photograph of the fabricated prototype.

A free space technique in an anechoic chamber is employed to measure the fabricated sample. Two broadband antennas are employed to transmit and receive signals in a 1–18 GHz band, connected to a vector network analyzer (Agilent E5063A) with a phase-stable cable. In the experiment, the reflection of a metal plate with an area similar to that of the sample is first measured for calibration and normalization of the MMAs.

Table 2. Comparison of the proposed absorber with other broadband absorbers.

Absorber structure	−10 dB bandwidth in GHz (%)	Operation spectrum (GHz)	Polarization insensitivity	FoM
Ref. [22]	60(150%)	10–70	No	0.175
Ref. [23]	8.8(71.9%)	8.2–17.4	Yes	0.199
Ref. [24]	8.6(82.7%)	6.06–14.66	Yes	0.173
Ref. [25]	12.6(86%)	8.4–21	No	0.170
This work	34.3(156.7%)	4.73–39.04	Yes	0.171

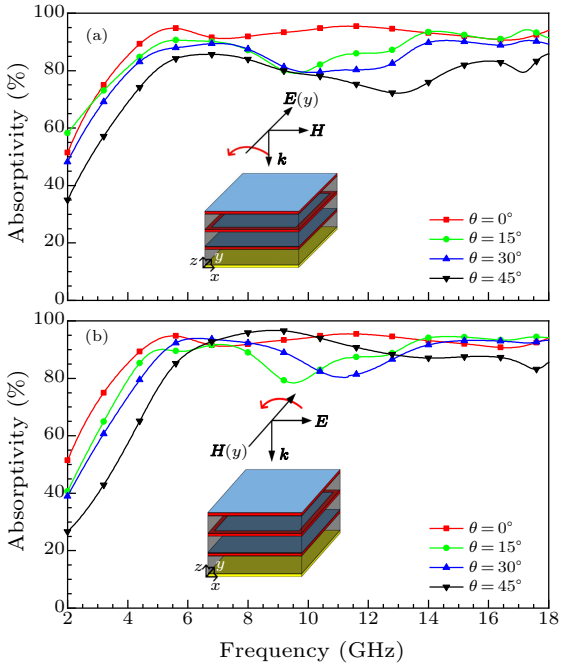

Fig. 6. Measured absorptivity spectra for the proposed structure under incidence angles from 0° to 45° for (a) TE polarization, and (b) TM polarization waves. The polarization direction and the incident angle θ are shown in the insets.

The measured absorptivity is shown in Fig. 6. Due to the limitations of the experimental device, the reflectivity is only measured in the 2–18 GHz band. As shown in Fig. 6, the absorption efficiency for both TE and TM waves is more than 90% in the range from 4.96 GHz to 18 GHz, under normal incidence.

However, the measured absorption band tends to shift to high frequencies as compared with the simulated results. This may be due to the samples' fabrication flaws and the resistance deviation from the ideal value for the resistive films. Nevertheless, both results are in good agreement.

In summary, we have presented an ultra-wideband multi-layer metamaterial absorber, which is polarization insensitive and angularly stable. A multilayered structure is constructed to achieve broadband absorption, with resistive films being utilized to enhance the impedance matching and provide high ohmic loss. Accordingly, more than 90% absorptivity from 4.73 GHz to 39.04 GHz can be achieved via the proposed absorber under normal illumination. Furthermore, the structure also provides angular stability, and is not sensitive to polarization. An equivalent circuit model is employed to evaluate the absorption mechanism. The experimental results are compatible with those of the simulation, demonstrating the absorber's efficiency in many real-world applications.

References

[1] Fallahi A, Yahaghi A, Benedickter H R *et al.* 2010 *IEEE Trans. Antennas Propag.* **58** 4051
[2] Kurihara H, Hirai Y, Takizawa K *et al.* 2005 *IEICE Trans. Electron.* **125** 2350
[3] Okano Y, Ogino S and Ishikawa K 2012 *IEEE Trans. Microwave Theory Tech.* **60** 2456
[4] Thomassin J, Huynen I, Jerome R *et al.* 2010 *Polymer* **51** 115
[5] Liu T, Cao X, Gao J *et al.* 2013 *IEEE Trans. Antennas Propag.* **61** 1479
[6] Salisbury W W 1952 *US Patent 2599944*
[7] Meshram M R, Agrawal N K, Sinha B *et al.* 2004 *J. Magn. Magn. Mater.* **271** 207
[8] Park M J and Kim S S 2000 *IEEE Trans. Magn.* **36** 3272
[9] Smith D R, Padilla W J, Vier D C *et al.* 2000 *Phys. Rev. Lett.* **84** 4184
[10] Chen H, Wu B, Zhang B *et al.* 2007 *Phys. Rev. Lett.* **99** 63903
[11] Zhang C, Yang J, Yuan W *et al.* 2017 *J. Phys. D* **50** 444002
[12] Yan M Y, Xu B J, Sun Z C *et al.* 2020 *Chin. Phys. Lett.* **37** 067801
[13] Xie S H, Fang X S, Li P Q *et al.* 2020 *Chin. Phys. Lett.* **37** 054301
[14] Han M K, Yin X W, Wu H *et al.* 2016 *ACS Appl. Mater. & Interfaces* **8** 21011
[15] Xie Y M, Liu C Y, Ding Z J *et al.* 2016 *Chin. Phys. Lett.* **33** 094208
[16] Hu J G, Xie W Q, Chen J X *et al.* 2020 *Opt. Express* **28** 22095
[17] Nizamani B, Salam S, Jafry A A A *et al.* 2019 *Chin. Phys. Lett.* **36** 074203
[18] Zhou K, Cheng Q, Song J L *et al.* 2019 *Opt. Lett.* **44** 3430
[19] Zhang C, Yang J, Yang L X *et al.* 2020 *Nanophotonics* **9** 2771
[20] Hu J G, Liu W, Xie W Q *et al.* 2019 *Opt. Lett.* **44** 5642
[21] Zhang C, Yang J, Cao W K *et al.* 2019 *Photon. Res.* **7** 478
[22] Sun J B, Liu L Y, Dong G Y *et al.* 2011 *Opt. Express* **19** 21155
[23] Zhang C, Cheng Q, Yang J *et al.* 2017 *Appl. Phys. Lett.* **110** 143511
[24] Sheokand H, Ghosh S K, Singh G *et al.* 2017 *J. Appl. Phys.* **122** 105105
[25] Xiong H, Hong J S, Luo C M *et al.* 2013 *J. Appl. Phys.* **114** 064109
[26] Shui W C, Li J M, Wang H *et al.* 2020 *Adv. Opt. Mater.* **8** 2001120
[27] Hu J G, Qing Y M, Yang S Y *et al.* 2017 *J. Opt. Soc. Am. B* **34** 861
[28] Arik K, Abdollahramezani S, Farajollahi S *et al.* 2016 *Opt. Commun.* **381** 309
[29] Liu P W and Lan T 2017 *Appl. Opt.* **56** 4201
[30] Langley R J and Parker E A 1982 *Electron. Lett.* **18** 294
[31] Chung Y C, Lee K W, Hong I P *et al.* 2011 *IEICE Electron. Express* **8** 89
[32] Zhao J, Zhang C, Cheng Q *et al.* 2018 *Appl. Phys. Lett.* **112** 73504